Supplemental Data

Mre11 Nuclease Activity Has Essential

Roles in DNA Repair and Genomic

Stability Distinct from ATM Activation

Jeffrey Buis, Yipin Wu, Yibin Deng, Jennifer Leddon, Gerwin Westfield, Mark Eckersdorff, JoAnn M. Sekiguchi, Sandy Chang, and David O. Ferguson

Supplemental Experimental Procedures

Generation of *Mre11*^{H129N} allele

The targeting construct used plasmid PLN-TK as backbone (Gorman et al., 1996). Targeting arms were generated by PCR with genomic DNA from TC1 mouse ES cells as template. A 4.0 kb region surrounding and including nuclease motif III was initially isolated in three separate PCR fragments each cloned into T-easy plasmid (Promega). A .9 kb fragment containing motif III underwent mutagenesis using the QuikChange Site-Directed Mutagenesis kit (Stratagene) for the C to A mutation, and a unique intronic HindIII site was filled-in using Klenow polymerase and subsequent ligation to generate a restriction fragment length polymorphism during southern blot analyses. The .9 kb fragment was ligated to adjacent 1.1 kb fragment to generate the upstream targeting arm, while the downstream arm derived from a single 2.0 kb PCR product. Targeting arms were sequenced entirely. 50 ug PvuI linearized plasmid was electroporated into TC-1 mouse embryonic stem cells (Deng et al., 1996).

One thousand G418 - gancyclovir double resistant colonies were screened by southern blot. Three targeted clones were obtained, one of which is shown (Figure 1c). Spectral karyotyping showed two of the three clones had a normal karyotype (data not shown) (Liyanage et al., 1996). The two targeted ES clones with normal karyotypes were transiently transfected with a plasmid expressing the Cre recombinase from a CMV promoter (Monroe et al., 1999). One hundred colonies from each targeted clone were screened by Southern blotting for deletion of the Neo^r gene. Four clones lacking *Neo*^{r} from each original clone were expanded (Figure 1C). Two clones were chosen for blastocyst injections and both yielded high contribution male chimeras which were subsequently mated to wild type 129sv females (Jackson Labs).

The presence of the H129N mutation, the blunted HindIII site, the remaining LoxP site, and the absence of undesired mutations were confirmed by sequencing cloned PCR products spanning the targeted region (data not shown).

The presence of the C to A mutation in total RNA from liver of three *Mre11*$^{H129N/+}$ mice was confirmed through sequencing cloned RT-PCR products. 8 of 15 cDNAs from *Mre11*$^{H129N/+}$ contained the mutant AAT asparagine codon, while 18 of 18 from *Mre11*$^{+/+}$ contained the wildtype CAT histidine codon.

Protein extracts from the same livers showed no aberrant sized Mre11 proteins by Western blot analysis (Figure S1A), and no difference in Mre11 protein levels by quantitation of Western blot signals using an infrared quantitative imaging system (Li-CORE odyssey system).

Therefore, our targeting strategy succeeded in generating the desired genomic changes without altering the locus in unintended ways.

A cohort of *Mre11*$^{H129N/+}$ mice and wildtype littermates were maintained in a pathogen free environment and observed for differences in lifespan, overall health, and fertility. After more than one year, no impact of *Mre11*^{H129N} heterozygosity has been observed. (Figure S1B and C, unpublished observations).

Generation of murine Mre11 germline conditional and null alleles

We employed a targeting strategy nearly identical to that described above for the nuclease deficient allele. The same targeting vector was used, except no mutations were present in exon 5, and a LoxP site was inserted at the HindIII site that was rendered blunt in the H129N targeting vector (Figure 1B). This generated a vector containing three LoxP sites, in which exon 5 and the *Neo*^{r} gene are each flanked by LoxP sites (floxed) (Figure 2A). Hypothetical splicing around deleted exon 5 to exon 6 would shift the reading frame and generate multiple stop codons after 8 amino acids. Deletion of the floxed region of the *Mre11* genomic locus in a cell line was shown previously to yield no detectable full length or truncated Mre11 protein (Xiao and Weaver, 1997). Southern blot and PCR approaches described above in generation of the Mre11^{H129N} allele (Figure 1B, C and D) indicated that two independent targeted clones were obtained (data not shown). Both yielded germline transmission in mice, which were mated to mice expressing the Cre recombinase in the germline from the EIIa promoter. Various recombinants of the three LoxP sites were identified in offspring using a PCR strategy (Figure 2B and C, and data not shown). Offspring with deletion of the *Neo*^{r} gene and preservation of the two LoxP sites within *Mre11* genomic sequences harbored the *Mre11* conditional (*Mre11*^{Cond}) allele, while those with deletion of *Neo*^{r} and the genomic locus harbored the *Mre11* null (*Mre11*$^{\Delta}$) allele. The organization of the modified Mre11 loci in these founder mice was confirmed by sequencing cloned PCR products spanning the region. The *Mre11* null (*Mre11*$^{\Delta}$) allele was confirmed in the same manner.

PCR based genotyping

PCR primers used for distinguishing the four Mre11 alleles (depicted in figure 2B) are as follows;

(A) 5' - TAC AAA AGG TTG AAA ATT TGA GAA GC - 3' (also named HinDLoxup1).

(D) 5' - TGT AAT TGC AGG TCC TTA AAG GC - 3' (also named BglLoxD1).

The unique band for each allele is;

Mre11^{WT} - 693 bp, Mre11^{Cond} - 764 bp, Mre11$^{\Delta}$ - 198 bp, Mre11^{H129N} - 729 bp.

The presence of the Mre11^{Cond} allele, and distinction from the Mre11^{WT} and Mre11^{H129N} alleles, was occasionally confirmed by PCR (not shown) using primer (A) combined with

5' TAGGTAGCTACAAACATATATCTGC 3' (named HindLoxD1).

Band sizes are Mre11^{Cond} - 200 bp, Mre11^{H129N} - 170 bp, Mre11^{WT} - 166 bp, Mre11$^{\Delta}$ - no band.

Thermocycling conditions for the above reactions entailed 33 cycles of 96 C for 30s, 53 C for 30s, 72 C for 40 s.

Growth and analysis of MEFs

Replication defective adenovirus expressing the Cre recombinase was used as described (Anton and Graham, 1995). Primary MEFs were immortalized at P2 by transfection with pBsSVD2005 (SV40 large T antigen expression vector). AdCre and AdE, supplied by University of Michigan

Vector Core were used at MOIs from 100 to 500:1 with comparable results. MEFs were grown 3 days post infection and split once prior to experiments. Proliferation assays performed by plating 5x10^5 cells on 10cm dishes each passage every 3 days. Sensitivity to ionizing radiation was performed as previously described (Rooney et al., 2002). Cellular senescence as measured by SA-β-Gal staining is described (Dimri et al., 1995).

G2/M checkpoint

7.5×10^5 MEFs were plated on 10 cm dishes, mock treated or irradiated 48 hours later with 10 Gy, and allowed to recover 1 hour. Flow cytometry (FC500 Beckman Coulter) for p-H3 (Ser10) staining (mitosis specific) (Van Hooser et al., 1998) was performed according to the manufacturer's instructions (Cell Signaling). Data was analyzed with FlowJo software Ver. 4.5.2 (Tree Star, Ashland, Oregon).

Western Blots and Immunofluorescence

Cell extracts were prepared in Laemmli buffer (4% SDS, 20% glycerol, 120 mM Tris-HCl, pH 6.8), proteins were resolved by SDS-PAGE and transferred using standard procedures. IR (10gy) treated MEFs were incubated 1 hr post IR. Antibodies described below. Retrovirus expression constructs for $TPP1^{\Delta RD}$, generation and infection of retroviral stocks of $TPP1^{\Delta RD}$, and Western Blot were performed as described (Guo, et al. 2007). Antibodies described below.

For Mre11 immunofluorescence, MEFs were grown on 2 chamber glass slides, treated with 10 gy of IR (^{137}Cs) with a 6 hr incubation post IR. MEFs were fixed in ice-cold methanol and permiablized with 1 X TBS, 0.5% triton X-100 at RT. Cells were blocked in TBS with 10% donkey serum, incubated overnight at 4°C with polyclonal Mre11 antibody (1:100, Cell Signaling), then incubated 1 hr with the secondary donkey anti-rabbit Cy2 conjugated antibody (1:200, Jackson Immunoresearch)

For NBS1 immunofluorescence, MEFs were grown on 2 chamber glass slides, treated with 10 gy of IR (^{137}Cs) with a 2 hr incubation post IR. MEFs were fixed in 4% paraformaldehyde and permiablized with 1 X TBS, 0.5% triton X-100 at RT. Cells were blocked in TBS with 10% sheep serum, incubated overnight at 4°C with monoclonal rabbit NBS1 antibody (1:50, Cell Signaling), then incubated 1 hr with the secondary goat anti-rabbit Alexa Flour 555 antibody (1:200, Molecular Probes).

For RPA immunoflourscence, MEFs were grown on 2 chamber glass slides, treated with 10 gy of IR (^{137}Cs) with a 2 hr incubation post IR. MEFs washed with 20mM HEPES, 50mM NaCl, 3mM MgCl2, 300mM sucrose, 1% triton X-100 and fixed in ice cold methanol and permiablized with 1X PBS 0.5% triton X-100 at RT. Cells were blocked in PBS with 1% tween20, 3% BSA, and 10% sheep serum, incubated overnight at 4°C with mouse monoclonal RPA1 antibody(2.5μg/ml, Calbiochem), then incubated 1 hr with the secondary sheep anti-mouse FITC antibody (1:200, Sigma).

For Rad51 immunofluorescence, MEFs were grown on 2 chamber glass slides, treated with 10 gy of IR (^{137}Cs) with a 6 hr incubation post IR. MEFs were fixed in 4% paraformaldehyde and permiablized with 1 X TBS, 0.5% triton X-100 at RT. Cells were blocked in TBS with 10% FCS serum, incubated overnight at 4°C with polyclonal rabbit Rad51 antibody (51RAD01) (1:200, Santa Cruz), then incubated 1 hr with the secondary goat anti-rabbit Alexa Flour 555 antibody (1:1000, Molecular Probes).

Immunoprecipitation of Mre11 protein

Immunoprecipitations were performed using protein G sepharose beads (GE healthcare) with 2 mg of protein extract incubated with anti-Mre11 antibody (Cell Signaling) for 16 hours at 4° C. Western blots were performed as above with antibodies Rad50 (Bethyl) at 1:1000, NBS1 (Novus) at 1:2000, Mre11 (Novus) at 1:1000, Tubulin (Sigma) at 1:2000.

Antibodies

For Western blots in Figure 2C and 4B the following antibodies were used: Mre11 (Novus, polyclonal); NBS1 (Novus, polyclonal); Rad50 (Bethyl Labs, polyclonal); α-tubulin (AbCam, monoclonal); CHK2, clone 7 (Upstate); and SMC1-ser957 (Cell Signaling). Secondary antibodies used were IRDye800CW Conjugated goat anti-rabbit or anti-mouse (Li-Cor Biosciences). Images were taken with an Odyssey infra-red imaging system at 800nm. (Li-Cor Biosciences).

For Western blots in Figure 4D the antibodies used are as follows: p-ATM Ser 1981(no.200-301-400, Rockland); ATM (Sc-23922, Santa Cruz); Mre11 (no.4895 Cell Signaling); Chk2 (no. 611570, BD Biosciences); γ-tubulin, HA (Sigma); γ-H2AX (no. 05-636 Upstate); anti-53BP1 was a kind gift from Phil Carpenter, UTHMS.

Analysis of mouse Mre11 cDNA and protein

For reverse transcriptase-mediated PCR (RT-PCR), total RNA from adult mouse liver was prepared using trizol solution (Invitrogen) followed by reverse transcription (SuperscriptII-Invitrogen). *Mre11* cDNA was amplified using a poly dT primer in combination with primers located within the first upstream exons. cDNA products were cloned into T-easy vector (Promega) and sequenced. For Western blot, protein extracts from portions of the same mouse livers used for cDNA isolation were used. Antibody for Mre11 was used at 1:500 dilution (Novus, monoclonal), and tubulin at 1:2000 (Sigma).

Telomere dysfunction induced foci

TIF assay was performed as described (Guo, et al. 2007)(Takai et al., 2003). Cells were infected and selected for 7-10 days for stable expression of $TPP1^{\Delta RD}$. The cells were grown on 8-well glass chambers, fixed with 2% paraformaldehyde and permeabilized in 0.5% NP-40. Cells were blocked in PBG (0.2% [w/v] cold water fish gelatin [Sigma G-17765]; 0.5% BSA in PBS) and incubated with the antibodies in PBG: 53BP1, or γ-H2AX. Secondary antibodies against mouse or rabbit IgG were labeled with Alexa 488 (Molecular Probes). Tamra-$(TTAGGG)_3$ PNA telomere probe (Applied Biosystems) was utilized. DNA was counterstained with DAPI and slides were mounted in 90% glycerol/10% PBS containing 1 μg/mL p-phenylene diamine (Sigma). Digital images were acquired on a Nikon Eclipse 800 with x63 and x100 plan-apo objectives and photographed with a cooled CCD camera. CCD chip nonlinearities were removed by taking bias and dark current frames and the optical train flat fielded to eliminate vignetting. Individual raw images were taken through DAPI, Rhodamine and FITC narrowband filters and stacked in MetaMorph and PhotoShop CS were utilized to compose the final images. The linear histogram stretch was applied equally to all raw images before stacking to maintain the same degree of contrast enhancement in all images. Only cells with ≥ 5 γ-H2AX signals or 53BP1 foci (green) co-localized with telomere signal $(TTAGGG)_3$ (red) were scored.

Pulsed field gel electrophoresis
MEFs grown to 90% confluence were exposed to 80 Gy IR or 0.4 μM aphidicolin. Chef gel analyses performed as described (Kiltie and Ryan, 1997). Cells were solidified into 1% LMP agarose plugs, incubated with proteinase K (1mg/mL, 48 hrs, 56°C). Plugs were inserted into wells of 1% agarose gel, and run optimized for 1-4 Mb range on a Bio-Rad CHEF DRII , dried, stained with Sybr green 1 (Invitrogen), imaged on a Typhoon 9400 imager (GE HealthCare) and quantified with ImageQuant software (GE Healthcare).

DR-GFP HDR Assay - Performed as described (Pierce et al., 1999). The previously described DR-GFP (kind gift of Dr. Maria Jasin) was integrated into the genome of MEFs via transfection with FuGene 6 (Roche) and colonies were selected with puromycin. Integration was confirmed by Southern blot. I-Sce was transiently expressed via infection with an I-Sce containing adenovirus (AdNGUS24i - kind gift of Drs. Frank Graham and Philip Ng) and MEFS were examined by flow cytometry 2 days after infection. Flow cytometry was carried out on a Beckman Coulter Flow Cytomics FC 500. Data was analyzed using Flow Jo 8.4.6 software.

V(D)J transient assay - Assays were performed as previously described (Rooney et al., 2003). In brief, 1 x 10^6 MEF cells were plated onto 10-cm dishes and allowed to attach for 24 h. Full-length RAG-1 and RAG-2 expression constructs and the pJH290 coding joining or pJH200 RS joining substrate plasmids were transfected into the cells using the Superfect kit (Qiagen). The cells were harvested 48 h after transfection and the plasmids were isolated by alkaline lysis and then electroporated into *Escherichia coli* MC1061. V(D)J recombination efficiencies were determined by calculating the ratio of 250 μg/ml ampicillin- and 10 μg/ml chloramphenicol-resistant colonies to ampicillin-resistant colonies.

Supplemental Acknowledgments

We thank the following; Jessica Knowlton for technical assistance. Dr. David Weaver for the 5' Southern blot probe in plasmid pYX1, Elizabeth Hughes, Keith Childs, and Galina Gavrilina under the direction of Dr. Thomas Saunders for the preparation of gene-targeted Mre11$^{H129N/+}$ and Mre11$^{Cond/+}$ ES cells and chimeric mice in the University of Michigan's Transgenic Animal Model Core, Dr Andras Nagy, Reka Nagy and Wanda Abramow-Newerly for their generosity in providing the R1 ES cell line, the University of Michigan Sequencing Core under direction of Dr. Robert H. Lyons.

Supplemental References

Anton, M., and Graham, F.L. (1995). Site-specific recombination mediated by an adenovirus vector expressing the Cre recombinase protein: a molecular switch for control of gene expression. Journal of virology *69*, 4600-4606.

de Lange, T. (2005). Shelterin: the protein complex that shapes and safeguards human telomeres. Genes Dev *19*, 2100-2110.

Deng, C., Wynshaw-Boris, A., Zhou, F., Kuo, A., and Leder, P. (1996). Fibroblast growth factor receptor 3 is a negative regulator of bone growth. Cell *84*, 911-921.

Dimri, G.P., Lee, X., Basile, G., Acosta, M., Scott, G., Roskelley, C., Medrano, E.E., Linskens, M., Rubelj, I., Pereira-Smith, O., *et al.* (1995). A biomarker that identifies senescent human cells in culture and in aging skin in vivo. Proc Natl Acad Sci U S A *92*, 9363-9367.

Gorman, J.R., van der Stoep, N., Monroe, R., Cogne, M., Davidson, L., and Alt, F.W. (1996). The Ig(kappa) enhancer influences the ratio of Ig(kappa) versus Ig(lambda) B lymphocytes. Immunity *5*, 241-252.

Kiltie, A.E., and Ryan, A.J. (1997). SYBR Green I staining of pulsed field agarose gels is a sensitive and inexpensive way of quantitating DNA double-strand breaks in mammalian cells. Nucleic Acids Res *25*, 2945-2946.

Liyanage, M., Coleman, A., du Manoir, S., Veldman, T., McCormack, S., Dickson, R.B., Barlow, C., Wynshaw-Boris, A., Janz, S., Wienberg, J., *et al.* (1996). Multicolour spectral karyotyping of mouse chromosomes. Nat Genet *14*, 312-315.

Monroe, R.J., Seidl, K.J., Gaertner, F., Han, S., Chen, F., Sekiguchi, J., Wang, J., Ferrini, R., Davidson, L., Kelsoe, G., *et al.* (1999). RAG2:GFP knockin mice reveal novel aspects of RAG2 expression in primary and peripheral lymphoid tissues. Immunity *11*, 201-212.

Pierce, A.J., Johnson, R.D., Thompson, L.H., and Jasin, M. (1999). XRCC3 promotes homology-directed repair of DNA damage in mammalian cells. Genes Dev *13*, 2633-2638.

Rooney, S., Alt, F.W., Lombard, D., Whitlow, S., Eckersdorff, M., Fleming, J., Fugmann, S., Ferguson, D.O., Schatz, D.G., and Sekiguchi, J. (2003). Defective DNA repair and increased genomic instability in Artemis-deficient murine cells. J Exp Med *197*, 553-565.

Rooney, S., Sekiguchi, J., Zhu, C., Cheng, H.L., Manis, J., Whitlow, S., DeVido, J., Foy, D., Chaudhuri, J., Lombard, D., *et al.* (2002). Leaky Scid phenotype associated with defective V(D)J coding end processing in Artemis-deficient mice. Mol Cell *10*, 1379-1390.

Takai, H., Smogorzewska, A., and de Lange, T. (2003). DNA damage foci at dysfunctional telomeres. Curr Biol *13*, 1549-1556.

Van Hooser, A., Goodrich, D.W., Allis, C.D., Brinkley, B.R., and Mancini, M.A. (1998). Histone H3 phosphorylation is required for the initiation, but not maintenance, of mammalian chromosome condensation. J Cell Sci *111 (Pt 23)*, 3497-3506.

Xiao, Y., and Weaver, D.T. (1997). Conditional gene targeted deletion by Cre recombinase demonstrates the requirement for the double-strand break repair Mre11 protein in murine embryonic stem cells. Nucleic Acids Res *25*, 2985-2991.

Table S1. Mre11$^{H129N/H129N}$ causes embryonic lethality

	number observed	(expected)	
Mre11 genotype	Live born	E13.5	E10.5
+ / +	147	24	14
+ / H129N	214	36	22
H129N / H129N	0	0	0
Total analyzed	361	60	36

Table S2. p53 deficiency does not rescue Mre11$^{H129/H129N}$ lethality

Mre11 genotype	p53	genotype	
LIVE BORN	+/+	+/-	-/-
+ / +	19	24	16
+ / H129	27	37	21
H129N / H129N	0	0	0
DAY E13.5	+/+	+/-	-/-
+ / +	5	13	9
+ / H129	18	24	12
H129N / H129N	0	0	0
DAY E9.5	+/+	+/-	-/-
+ / +	5	13	6
+ / H129	7	14	11
H129N / H129N	2	5	4

Table S3. Spontaneous chromosomal anomalies in primary and immortalized Mre11 deficient MEFs (DAPI staining)

Genotype	Mre11$^{+/\Delta}$	Mre11$^{+/\Delta}$	Mre11$^{\Delta/\Delta}$	Mre11$^{\Delta/\Delta}$	Mre11$^{H129N/\Delta}$	Mre11$^{H129N/\Delta}$	Mre11$^{+/+}$	Mre11$^{Cond/\Delta}$	Lig4-/-
Cell type	Primary MEFS AdCre	Immortal MEFS AdCre	Primary MEFS AdCre	Immortal MEFS AdCre	Primary MEFS AdCre	Immortal MEFS AdCre	Primary MEFS No Virus	Immortal MEFS AdE	Immortal MEFS AdCre
Total Metaphases	110	105	122	124	123	115	60	46	80
Chromatid Gaps/Breaks	13 (0.12)	6 (0.057)	160 (1.31)	178 (1.43)	187 (1.52)	156 (1.36)	6 (0.1)	8 (0.17)	5 (0.06)
Fragments	24 (0.22)	17 (0.16)	175 (1.43)	145 (1.17)	167 (1.36)	150 (1.30)	10 (0.17)	4 (0.09)	66 (0.83)
Fusions (dicentrics)	1 (0.01)	1 (0.01)	10 (0.08)	7 (0.06)	6 (0.05)	5 (0.05)	0 (0)	0 (0)	1 (0.01)
Radials	1 (0.01)	0 (0)	14 (0.11)	15 (0.12)	19 (0.15)	10 (0.09)	0 (0)	0 (0)	0 (0)
Total anomalies	39	24	359	345	379	321	16	13	72
Anomalies per metaphase	0.35 ± 0.1	0.23 ± 0.1	2.91 ± 0.4	2.72 ± 0.3	3.09 ± 0.4	2.79 ± 0.4	0.26 ± 0.1	0.28 ± 0.1	0.9 ± .2

Table S4. Spontaneous chromosomal anomalies in Mre11 deficient MEFs analyzed by SKY and DAPI

Genotype	$Mre11^{+/\Delta}$	$Mre11^{\Delta/\Delta}$	$Mre11^{H129N/\Delta}$
Total Metaphases	29	40	36
Chromatid Gaps/breaks	7	82	71
Non-homologous Fusions	0	4	2
Homologous fusions	0	2	2
Translocations	2	25	31

Table S5. Chromosomal anomalies after recovery from IR exposure

Genotype	**$Mre11^{+/\Delta}$**			**$Mre11^{\Delta/\Delta}$**			**$Mre11^{H129N/\Delta}$**			**$Lig4^{-/-}$**		
Time of recovery	**24hr**	**48hr**	**72hr**	**24hr**	**48hr**	**72hr**	**24hr**	**48hr**	**72hr**	**24hr**	**48hr**	**72hr**
Metaphases	30	30	30	30	30	30	30	30	30	30	30	30
Fragments	28	21	14	57	67	65	75	89	80	240	203	251
Gaps/Breaks	1	0	0	24	30	29	29	27	29	20	24	24
Fusions (dicentrics)	0	1	0	17	19	20	13	11	13	21	20	18
Total Anomalies	29	22	14	98	116	114	117	127	122	281	284	293
Metaphases with Damage	17	15	8	25	26	27	27	27	26	29	28	29
%of Metaphases with Chromosomal anomalies	57%	50%	27%	83%	87%	90%	90%	90%	87%	97%	93%	97%

Table S6. Chromosomal anomalies after treatment with aphidicolin and recovery

Genotype	$Mre11^{+/\Delta}$	$Mre11^{+/\Delta}$	$Mre11^{\Delta/\Delta}$	$Mre11^{\Delta/\Delta}$	$Mre11^{H129N/\Delta}$	$Mre11^{H129N/\Delta}$	$Lig4^{-/-}$	$Lig4^{-/-}$
Time of recovery	No recovery	72 Hr recovery	No recovery	72 Hr recovery	No recovery	72 Hr recovery	No recovery	72 Hr recovery
Metaphases	25	25	25	25	25	25	25	25
Gaps	29	20	43	57	45	53	40	46
Fragments	29	57	60	151	54	187	63	61
Fusions (dicentrics)	1	4	8	46	7	39	2	9
Radials	0	0	8	23	5	17	1	2
Total anomalies	59	81	119	277	111	296	106	122
Anomalies per metaphase	2.36	3.24	4.76	11.08	4.44	11.84	4.24	4.88
Shattered Metaphases (unscored)	0	0	0	2	0	3	0	0

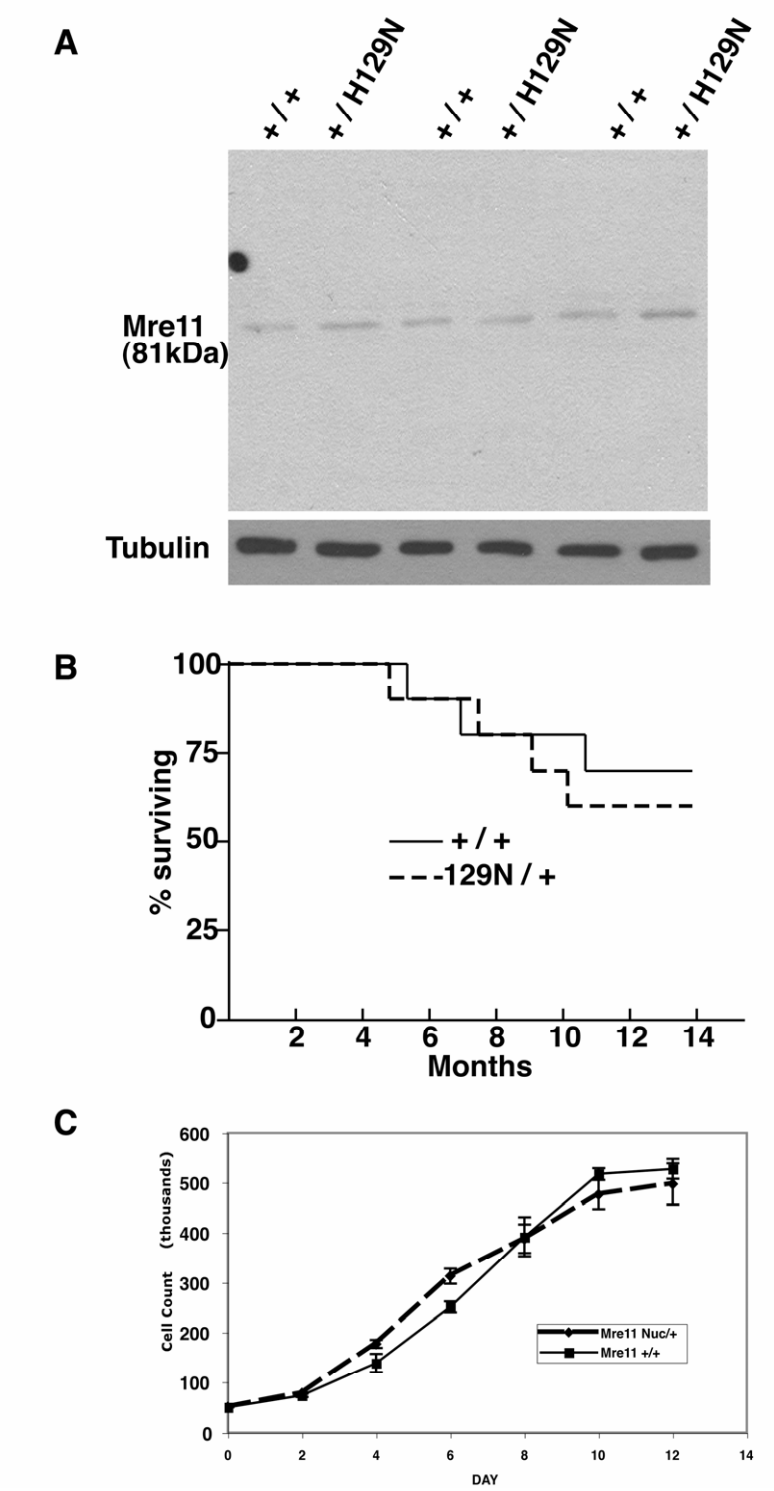

Figure S1. Mre11^{H129N} heterozygosity confers no obvious phenotype.
(A) Western blot analysis for Mre11 protein comparing fibroblasts from *Mre11*$^{+/+}$ and *Mre11*$^{H129N/+}$ mice. Each pair shown were littermates. Tubulin was used as loading control. (B) *Mre11*$^{+/+}$ and *Mre11*$^{H129N/+}$ mice have indistinguishable life spans up to one year of age. (C) Growth curves of primary MEFs.

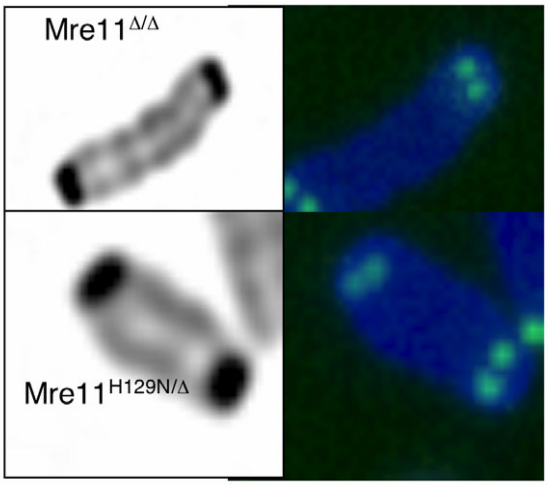

Figure S2. Dicentric chromosomes in *Mre11*$^{\Delta/\Delta}$ and *Mre11*$^{H129N/\Delta}$ metaphases. Note absence of telomere (TTAGGG) PNA-FISH signals (green on right) within the fused long arms (grey-left, blue-right). Telomere signals are apparent on non-fused short arms adjacent to centromeres (dark DAPI staining-left). Telomere dysfunction may manifest as chromosome fusions due to ligation of telomeres mistaken for DSBs (de Lange, 2005). To determine if fusions arising in the Mre11 deficiencies possess telomeric sequences we employed a telomere specific FISH probe. Telomere signal was not detected in the fused long arms of dicentric chromosomes (*Mre11*$^{\Delta/\Delta}$ 0/7, *Mre11*$^{H129N/\Delta}$ 0/6). Therefore, these dicentric chromosomes likely arise by mechanisms other than telomere dysfunction. While it is a formal possibility that repeats below the level of detection could be present in some cases, our data nonetheless argue against a major role for MRN in telomere protection *per se*.

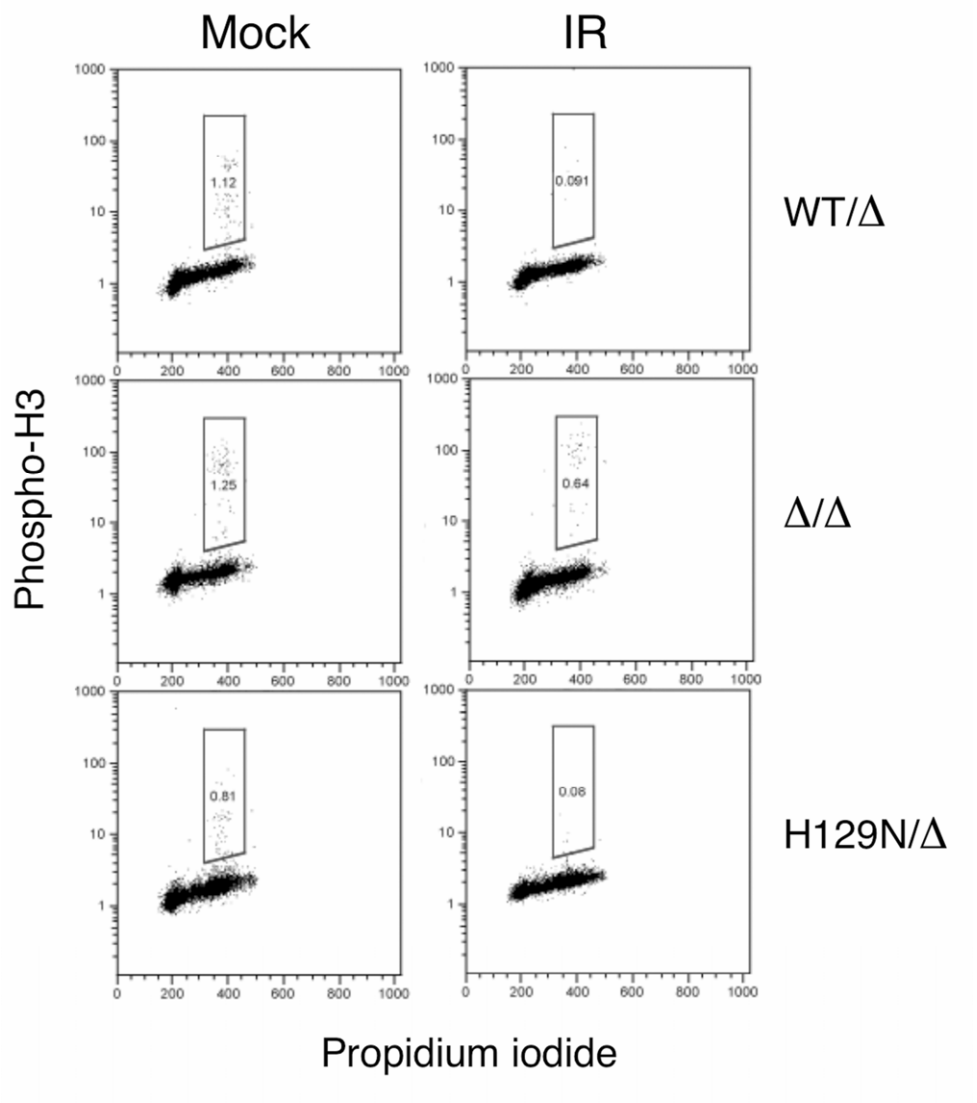

Figure S3. Flow cytometric analysis for phospho-H3 staining. phospho-H3 staining is presented on the Y axis, and propidium iodide (PI) on the X axis, reflecting DNA content. The gate encompassing cells committed to M phase is shown in each plot.

pJH290 Coding Joint (Hairpin)

	Deletions	Deletions
	+/Δ	
	Upstream	Downstream
1	-3	-4
2	-2	-1
3	-3	-2
4	-3	-4
5	-2	-5
6	-3	-1
7	-4	0
8	-1	0
9	-6	-4

	H129N/Δ	
	Upstream	Downstream
1	-5	-6
2	-4	-3
3	-3	-4
4	0	-7
5	-4	-9
6	-6	-4
7	-2	-5
8	-2	-6
9	-1	-2
10	-5	-5

	Δ/Δ	
	Upstream	Downstream
1	-3	-2
2	-2	-1
3	-4	-4
4	-1	-8
5	-4	-4
6	-5	-4
7	-2	-5
8	-2	-1

pJH200 Sigal Joint (Blunt)

	Deletions	Deletions
	+/Δ	
	Upstream	Downstream
1	0	0
2	0	0
3	0	0
4	0	0
5	0	0
6	0	0
7	0	0
8	0	0
9	0	0
10	0	0
11	0	0
12	0	0

	H129N/Δ	
	Upstream	Downstream
1	0	0
2	0	0
3	0	0
4	0	0
5	0	0
6	0	0
7	0	0
8	0	0
9	0	0
10	0	0
11	0	0

	Δ/Δ	
	Upstream	Downstream
1	0	0
2	0	0
3	0	0
4	0	0
5	0	0
6	0	0
7	0	0
8	0	0
9	0	0
10	0	0
11	0	0

Figure S4.

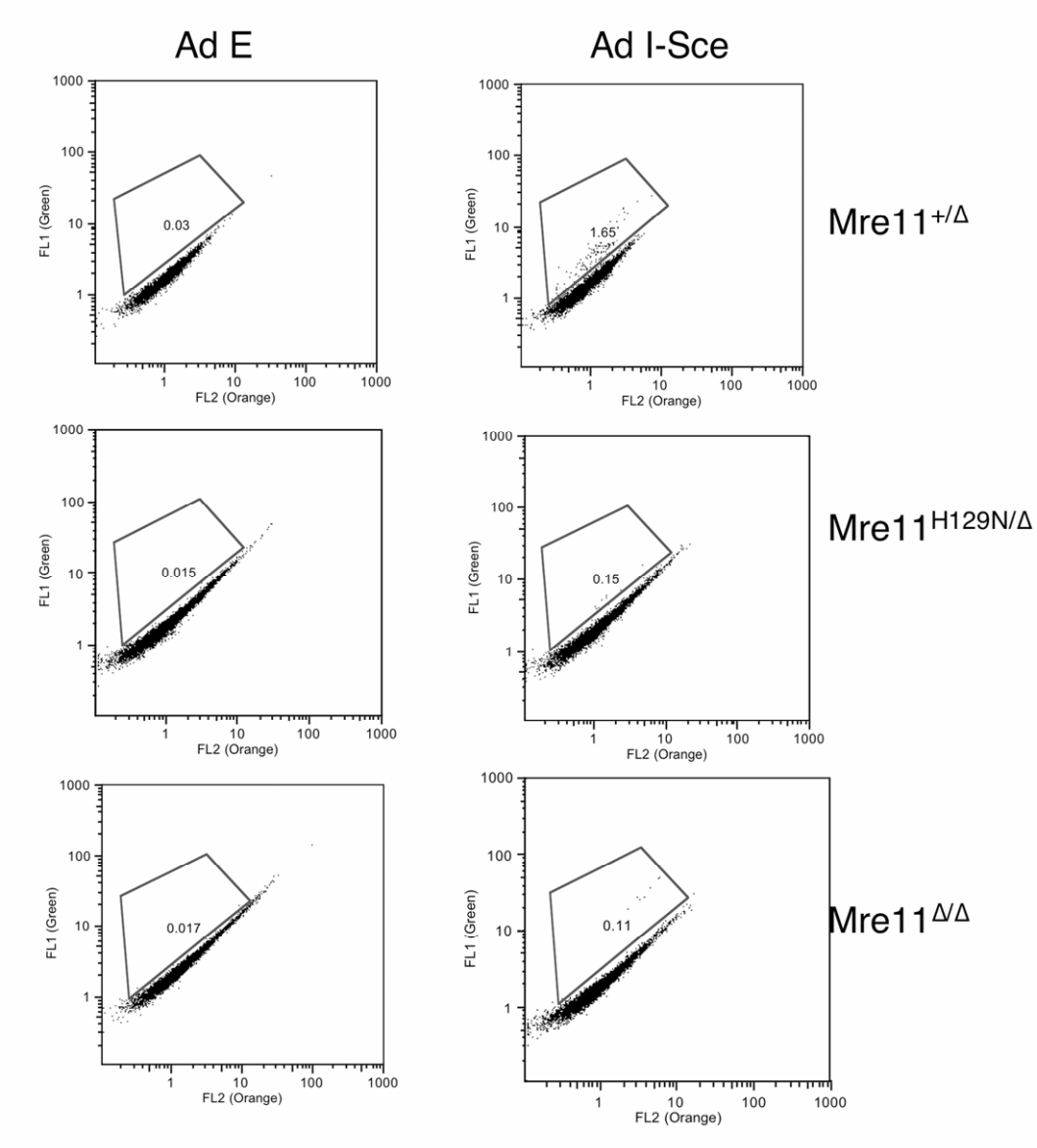

Figure S5. MEFs carrying one intact copy of substrate DRGFP were analyzed by flow cytometry. Representative flow cytometric analysis for HDR in MEFs after I-*Sce*I expression is shown. The GFP-positive population, reflecting HDR repair events, is isolated within the gate. FL1, green fluorescence; FL2, orange fluorescence. Events outside the gate, which are equivalent with or without I-SceI, represent autoflourscence.